International Journal of Mechanical, Industrial and Aerospace Sciences
ISSN: 2517-9950
Vol:7, No:7, 2013

# Some Studies on Temperature Distribution Modeling of Laser Butt Welding of AISI 304 Stainless Steel Sheets

N. Siva Shanmugam, G. Buvanashekaran, and K. Sankaranarayanasamy

***Abstract*—**In this research work, investigations are carried out on Continuous Wave (CW) Nd:YAG laser welding system after preliminary experimentation to understand the influencing parameters associated with laser welding of AISI 304. The experimental procedure involves a series of laser welding trials on AISI 304 stainless steel sheets with various combinations of process parameters like beam power, beam incident angle and beam incident angle. An industrial 2 kW CW Nd:YAG laser system, available at Welding Research Institute (WRI), BHEL Tiruchirappalli, is used for conducting the welding trials for this research. After proper tuning of laser beam, laser welding experiments are conducted on AISI 304 grade sheets to evaluate the influence of various input parameters on weld bead geometry i.e. bead width (BW) and depth of penetration (DOP). From the laser welding results, it is noticed that the beam power and welding speed are the two influencing parameters on depth and width of the bead. Three dimensional finite element simulation of high density heat source have been performed for laser welding technique using finite element code ANSYS for predicting the temperature profile of laser beam heat source on AISI 304 stainless steel sheets. The temperature dependent material properties for AISI 304 stainless steel are taken into account in the simulation, which has a great influence in computing the temperature profiles. The latent heat of fusion is considered by the thermal enthalpy of material for calculation of phase transition problem. A Gaussian distribution of heat flux using a moving heat source with a conical shape is used for analyzing the temperature profiles. Experimental and simulated values for weld bead profiles are analyzed for stainless steel material for different beam power, welding speed and beam incident angle. The results obtained from the simulation are compared with those from the experimental data and it is observed that the results of numerical analysis (FEM) are in good agreement with experimental results, with an overall percentage of error estimated to be within ±6%.

***Keywords*—**Laser welding, Butt weld, 304 SS, FEM.

## I. Introduction

LASER beam welding (LBW) is one of the most important manufacturing processes used for joining of materials. It is also a remarkably complicated process involves nonlinear operation with extremely high temperatures. Since its invention more than two decades ago, laser beam welding has been more of an art than a science. Laser beam welding is a high-power density welding process having a focus diameter of 0.2 to 1.0mm, resulting in a narrow Heat Affected Zone (HAZ). Hence the process results in lower distortion, residual stress and strain compared to the conventional welding [1]. It offers a number of attractive features such as weld bead with high depth-to-width ratio, reliability, repeatability and ability to automate with high throughput. During the laser welding process, a high energy beam ($10^5$ – $10^6$ W/cm$^2$) quickly melts the surface of a workpiece material. The beam then resulting in evaporation of the same and creates the keyhole with a plasma plume or cloud covering the keyhole area. The plasma plume expands to a variable extent, depending on the laser beam features, process input parameters and the surrounding atmosphere [2].

Over the last decade or so, a number of researchers have been working in the area of analytical as well as finite element based numerical simulation techniques to predict the temperature fields during laser beam welding process using the moving heat source model. Reference [3] considered a point source incident on, and moving relative to, an infinite material to simulate surface melt runs relating to conduction welding. He also derived the solution for an infinite line source extending through the depth of the materials, its axis perpendicular to the top and bottom surfaces. Reference [4] approximated Rosenthal's solution and predicted that the proportion of power needed to cause melting as a function of the incident power. Reference [5] evaluated numerically the spatial distribution of the temperature rise induced by a laser beam absorbed in a solid medium by reducing into a one dimensional model and provided a solution for a general laser intensity distribution for the case of a Gaussian beam. Further, he proposed a closed-form expression in terms of tabulated functions for the maximum temperature rise. Reference [6] proposed several two dimensional, numerical and analytical models of temperature profiles in the horizontal plane of laser welding with fluid flow. They assumed that the heat transfer and fluid flow are two dimensional and the keyhole is circular and isothermal. Reference [7] developed a simple algorithm for the calculation of the laser induced temperature field in a thin moving sheet. They also formed an asymptotic formula for predicting the temperature at large distance from heating point. However, the melting and/or evaporation were not

N. Siva Shanmugam is with the Department of Mechanical Engineering, National Institute of Technology, Tiruchirappalli 620015, Tamil Nadu, INDIA (corresponding author phone: +91-431-2503425; fax: +91-431-2500133; e-mail: nsiva@nitt.edu).

G. Buvanashekaran is with the Welding Research Institute, Bharat Heavy Electricals Limited, Tiruchirappalli 620014, Tamil Nadu, INDIA (e-mail: gbs@bheltry.co.in).

K. Sankaranarayanasamy is with the Department of Mechanical Engineering, National Institute of Technology, Tiruchirappalli 620015, Tamil Nadu, INDIA (e-mail: ksnsamy@nitt.edu).

considered in the above works. A mathematical model for the simulation of weld pool during deep penetration laser beam welding based on a numerical solution was presented by [8]. They developed a three dimensional simulation model in order to investigate the influence of the fluid dynamics in the fusion zone on the local temperature distribution. There are several research articles dealing with the temperature fields and shape of the fusion zone of laser beam welds related to different process parameters by using analytical solution, numerical models and experimental work. However, the effect of all influencing factors of laser welding on weld bead geometry has not been extensively studied. Still, more work is required in terms of conducting experimental trials and doing finite element simulation for understanding the combined effect of laser parameters on the temperature profiles and molten pool shape of austenitic stainless steel sheet.

In this research article, investigations are carried out to analyze the temperature profiles and molten pool shape in laser welding of 1.6 and 2.5mm thick AISI 304 stainless steel sheets using finite element transient heat transfer analysis. The results showed that the above said input process parameters have strong influence on the resulting temperature profiles during laser welding of austenitic stainless steel sheet. Experimental validations are also done to define these parameters correctly in order to establish quantitative as well as qualitative correlations between finite element simulations and experiments.

## II. Experimental Work

The experimental procedure involves a series of trials to develop and evaluate the knowledge base for laser welding of AISI 304 stainless steel sheets. Based on the weld bead geometry i.e. depth of penetration and bead width (observed through optical microscopy), the appropriate ranges of various input process parameters are selected for conducting future experimental trials.

### *A. Experimental Setup*

An industrial 2kW CW Nd:YAG laser system available at Welding Research Institute (WRI), BHEL, Trichy, Tamil Nadu, India is used commercially for welding on a wide range of carbon manganese steels, coated steels, stainless steels, aluminium alloys and titanium.

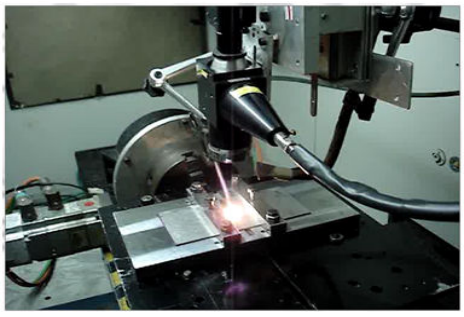

Fig. 1 Laser welding trials carried out at WRI

This laser system generates a continuous or high speed modulated output which can produce a continuous molten pool for high speed welding and deep penetration welding. It can be set to produce conduction-mode, penetration-mode and also keyhole-mode welding regimes similar to electron-beam welding. The welding system consists of a power source, laser head and the cooling unit. Fig. 1 shows the laser welding trials carried out on AISI 304 stainless steel sheet for predicting the weld bead geometry.

### *B. Butt- Joint Welds*

Laser seam experiments are carried out on AISI 304 stainless steel sheets of 1.6 and 2.5mm thicknesses using the parameters given in Table I. The selection of welding parameters is based on the results attained from the bead-on plate welding trials. The specimens are cut into small coupons of size of 100 x 100mm and the experiments are conducted for two different sheet thicknesses. Further, the specimens are prepared with due care to get the required alignment for the joint. Then, they are cleaned using sandblasting on the top and bottom surfaces to maximize the energy absorbed. From the previous published results of laser spot welding and bead-on plate trials, it is observed that the beam incident angle has shown a significant effect on weld bead geometry, particularly, a high depth of penetration is achieved for narrow beam incident angle of $85^{o}$ irrespective of the beam power, beam exposure time and welding speed. Hence, it is decided to conduct all the welding trials by keeping the beam incident angle as $85^{o}$. To protect the laser head and weld pool an industrial pure Argon gas (99.99%) with flow rate of 5litres/min is used as a shielding medium during the experimental trials.

TABLE I
Laser Welding Parameters for Butt Welding of AISI 304 Stainless Steel Sheets

| Sl. No. | Beam Power (BP), watts | Welding Speed (WS), mm/min | Beam Angle (BA), deg. | Focal Length (F), mm | Gas flow rate (GF), l/min |
|---|---|---|---|---|---|
| 1. | 1000 | 400 | | | |
| 2. | 1400 | 800 | 85 | 160 | 5 |
| 3. | 1800 | 1200 | | | |

### *C. Butt-Joint Results*

An image analyzer is used to analyze the top and bottom surface and to measure the weld bead geometry of each weld. Fig. 2 shows the comparison of weld bead geometries for bead-on plate welding and butt welding of 2.5mm thick AISI 204 stainless steel sheet for the beam power of 1400 W and welding speed of 400mm/min. It is noted that the depth and width of the welding seam for both the process is almost similar to each other with the aspect ratio of around 1.5. Hence it is appropriate that the results of bead-on plate welding (which is fairly easy to experiment) can be used for selecting laser process parameters for butt welding.

Fig. 3 shows the effects of beam power on laser-weld bead geometry of 2.5mm thick AISI 304 stainless steel sheet. It is noted that the weld dimensions, i.e. depth to width ratio have a significant change as the beam power is increased from 1000

to 1,800 W for the constant welding speed of 800mm/min. In addition to that, an increase in beam power from 1000 to 1,800 W shows a marked increase in depth of penetration from approximately 0.86 (at 1000 W) to 1.66mm (at 1,800 W). Similarly, there is also a slight increase in bead width from 0.98 (at 1000 W) to 1.38mm (at 1,800 W). The possible reason may be that the power density distribution of the laser beam increases as the beam power increases, and it covers a wider effective area on the top surface of the sheet. Therefore, there is a slight increase in the bead width of the laser weld.

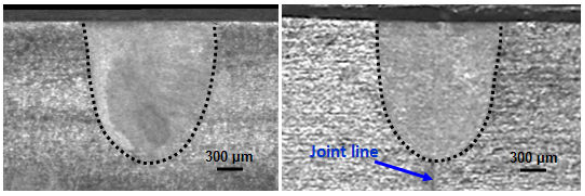


Fig. 2 Comparison of weld bead geometry for bead-on plate welding and butt welding

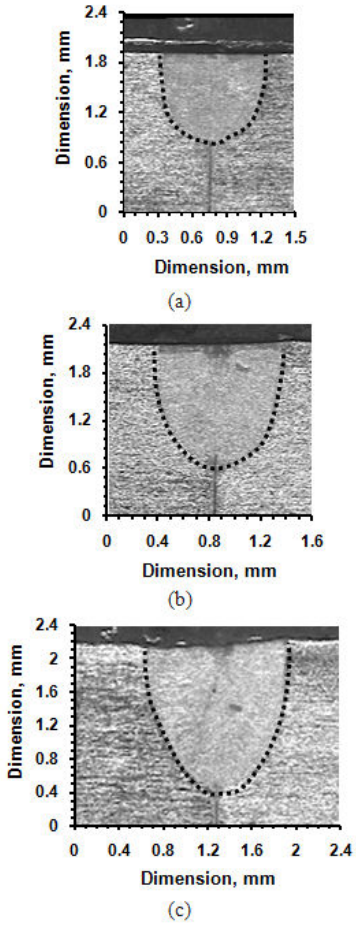


Fig. 3 Weld bead geometries for welding speed of 800mm/min, beam angle of 85° and beam power of (a) 1000W, (b) 1400W and (c) 1800W – Partial Penetration

Fig. 4 depicts the complete penetration for the 2.5mm thick base metal obtained for beam power equal to 1800 W at welding speed of 400mm/min and beam incident angle of 85°. The energy input for the beam power of 1800 W and welding speed of 400mm/min is high compared to other combinations of beam power and welding speed considered for this study. The weld bead observed through optical microscopy shows the characteristic of laser welding with depth/width ratio closer to 2. From the real color images of top and bottom surfaces of the weld shown in Fig. 5, a smooth weld bead profile on both sides of the specimen (top and root) with full penetration and without any discontinuity is observed.

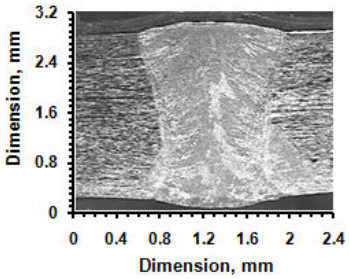


Fig. 4 Weld bead profile for beam power of 1800 W, welding speed of 400 mm/min and beam angle of 85° – Full Penetration

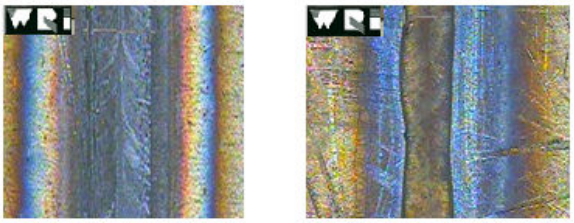

(a) (b)

Fig. 5 Smooth finish of Butt weld bead surfaces (a) Top side and (b) Root side

The results from Table II show that the dimensions of weld bead (depth to width ratio) as a function of beam power and welding speed. It can be seen that as the welding speed increases the depth-to-width ratio decreases irrespective of the beam power. This is due to the fact that the energy input to the base metal is decreased as the welding speed increases at constant beam power. If the energy input is low, conduction mode welding is the main mechanism involved which results in high conduction loses and produces low depth of penetration (low depth to width ratio). Once the energy input attains a high level (270 J/mm), a stable keyhole is formed, which enables the laser beam to penetrate deeply (high depth to width ratio) and deep penetration mode mechanism becomes predominant. Using the data presented in Table II, the input process parameter is selected for butt welding of 1.6 mm thick sheet. Fig. 6 shows the weld bead profile (top surface and shape of the bead) for butt welding of 1.6 mm thick AISI 304 stainless steel sheet using beam power of 1800 W and welding speed of 800mm/min. A smooth and uniform welded surface with sound face and root bead is observed in

the weld for the selected beam power and welding speed. This is possible due to the reason that the selected beam power and welding speed for this trial attains a linear energy input of 135J/mm which has the tendency to penetrate the 1.6mm thick sheet.

TABLE II
MEASURED WELD BEAD DIMENSIONS FOR BUTT WELDING

| Sl. No. | BP, Watts | WS, mm/min | Beam Energy (BE), J/mm | DOP, mm | BW, mm | Remarks (Welding of 2.5mm thick sheet) |
|---|---|---|---|---|---|---|
| 1. | 1000 | 400 | 150 | 1.78 | 1.42 | Partial Penetration |
| 2. | 1000 | 800 | 75 | 0.86 | 0.98 | Partial Penetration |
| 3. | 1000 | 1200 | 50 | 0.5 | 0.87 | Partial Penetration |
| 4. | 1400 | 400 | 210 | 2.1 | 1.4 | Partial Penetration |
| 5. | 1400 | 800 | 105 | 1.26 | 1.16 | Partial Penetration |
| 6. | 1400 | 1200 | 70 | 0.83 | 0.95 | Partial Penetration |
| 7. | 1800 | 400 | 270 | 2.5 | 1.45 | Full Penetration |
| 8. | 1800 | 800 | 135 | 1.66 | 1.38 | Partial Penetration |
| 9. | 1800 | 1200 | 90 | 1.33 | 1.2 | Partial Penetration |

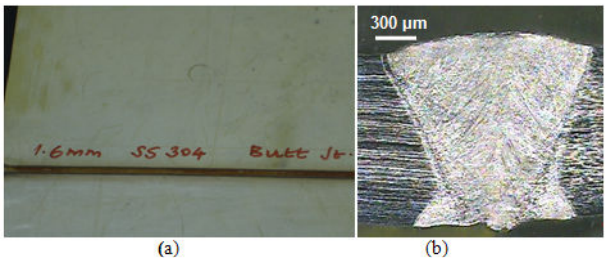


Fig. 6 Weld bead profile of 1.6mm thick stainless steel sheet (a) Top surface and (b) Weld bead shape

The experimental results reveal that the beam power and welding speed are the two process input parameters having a significant effect on weld bead geometry of butt weld of AISI 304 stainless steel sheets. Low welding speed and high beam power provides high linear energy input on the base metal and the formation of keyhole is stable resulting in deep penetration welds. The results indicate that penetration depth increases and decreases significantly with increase in beam power and welding speed, respectively. The increasing beam power leads to increased energy input causing more metal to melt and consequently, more penetration is achieved. However, the opposite phenomenon is observed for welding speed, as increased welding speed lessens the interaction time and hence, provides less time for the heat energy to flow deep into the material. Moreover, it is evident that various combinations of these parameters are possible to obtain the desired penetration depth. Therefore, it is concluded that the combination of higher beam power and lower welding speed needs to be selected within the specified range to obtain a good quality weld with deeper penetration.

## III. FINITE ELEMENT SIMULATION OF LASER WELDING PROCESS

Finite Element Simulation models of the welding process, which have been validated through experimental results, are of major importance for number of reasons: the deep understanding of the laser welding physics, the efficient definition of the laser welding process parameters and the reliable extension of the process applicability to modern demanding industrial requirements [9]. When developing the welding procedure for a given application, the laser parameters must be characterized and fully specified [10]. This is usually done by trial and error where the knowledge and experience of engineers play a major role.

To simulate the laser welding process, a three dimensional nonlinear transient thermal analysis is used. The commercial nonlinear finite element code, ANSYS is employed to solve the transient thermal analysis [11]. ANSYS is a general purpose finite element modeling package for numerically solving a wide variety of mechanical problems, used widely in industry to simulate the response of a physical system to structural loading, thermal and electromagnetic effects. ANSYS uses the finite-element method to solve the underlying governing equations and the associated problem-specific boundary conditions. It enables to simulate test in virtual environment before manufacturing prototypes of products.

### *A. Mathematical Model of Heat Transmission during Laser Welding Process*

In the view of present study, the laser beam is considered to be normally impinging onto the workpiece surface, along the z axis and it is translated with a constant welding speed, v, along the x axis. The heat exchange takes place between the base metal and its surroundings during welding and subsequently cooling takes place by both convection and radiation. This can be modelled by defining the convection coefficient h and surface emissivity ε in the FE simulation. In this model, the dependence of the local temperature change in the temperature field in its surrounding is considered. Locally supplied heat increases the local temperature according to the local volume-specific heat capacity cρ [J/mm3K]. More the unevenness of temperature distribution at a specific time more is the rapid change in material temperature [12]. For the homogeneous and isotropic continuum with temperature-dependent material characteristic (specific heat and thermal conductivity (k) change with temperature), the following field equation of heat conduction applies [13]:

$$\rho(T)c(T)\frac{\delta T}{\delta t} + v\rho(T)c(T)\frac{\delta T}{\delta x} = \frac{\delta}{\delta x}\left(k_x\frac{\delta T}{\delta x}\right) + \frac{\delta}{\delta y}\left(k_y\frac{\delta T}{\delta y}\right) + \frac{\delta}{\delta z}\left(k_z\frac{\delta T}{\delta z}\right) + \text{heat source} \quad (1)$$

where T is the body temperature ($^oC$), which is a function of x, y, z and time t in seconds (s), ρ is the density of the material (kg/mm$^3$), $k_x$, $k_y$ and $k_z$ are the thermal conductivity in the x, y and z directions, respectively, (W/mm$^oC$) and c is the specific heat capacity (J/kg$^oC$). The above said physical properties are temperature dependent. The heat source is expressed as heat generation per unit volume (J/mm$^3$). In modeling of heat transmission during welding, the effects of weld pool stirring are ignored.

*B. Material Model*

As discussed earlier, the materials to be joined are commercial AISI 304 stainless steel sheets of various thicknesses like 1, 1.6, 2.5 and 3.16mm. AISI 304 is a general-purpose austenitic stainless steel with a face centred cubic structure. The melting point of stainless steel ranges from 1400 to 1455°C. The solidified microstructure of AISI 304 comprises austenite and a dual phase austenite-ferrite mixture. Thermo-physical properties (temperature dependent) of the material are assumed to be isotropic and homogeneous and are taken according to [14]. The latent heat of fusion is 247 kJ/kg, to be released or absorbed over the range of temperature between $T_S$ = 1400°C and $T_L$ = 1500°C and the latent heat of vaporization is 7600 kJ/kg (above 2467°C) [15]. The chemical composition of selected AISI 304 stainless steel is listed in Table III.

TABLE III
AISI 304 STAINLESS STEEL CHEMICAL COMPOSITION

| Component | C | Cr | Fe | Mn | Ni | P | S | Si |
|---|---|---|---|---|---|---|---|---|
| **Wt. %** | 0.055 | 18.28 | 66.34 | 1.00 | 8.48 | 0.029 | 0.005 | 0.6 |

*C. Heat Source Model*

The key problem in performing the finite element analysis of laser welding is the modelling of welding heat source $Q_v(x,y,z)$. Literature review reveals that researches are in progress aiming at defining a reliable heat source for the laser welding process.

In laser welding process, a part of the energy generated by the laser source is lost before absorbed by the weld specimen. The energy loss is due to the reflection from the specimen surface while rest of the energy is absorbed by the specimen [16]. The energy loss for AISI304 stainless steel material determined experimentally by the past researchers [17] is 30.7% of the nominal power of the laser source [18]. Therefore, the absorbed energy considered for this present investigation is 69.3% of the beam power.

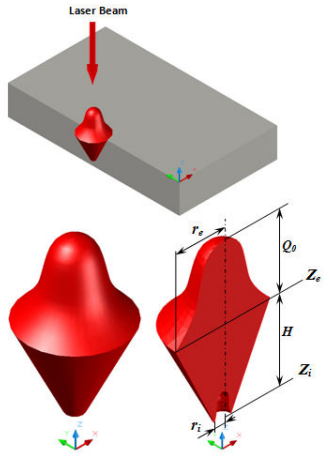


Fig. 7 Schematic of 3D Conical Heat source model

During simulation, consideration is given to the fact that the heat comprises a plane heat source on the top surface and a conical heat source along the thickness direction. In that 69.3% of the beam power, the power absorbed on the surface of the specimen is 17.3% $(Q_{surf})$ and the remaining 52.7% by the keyhole wall $(Q_{keyhole})$. Assuming that the laser beam maintains a constant Transverse Electromagnetic mode ($TEM_{00}$), the Gaussian heat flux distribution Q(x,y) can be expressed as:

$$Q(x,y) = \frac{3Q_{surf}}{\pi R^2}\exp\left(-\frac{3(x^2+y^2)}{R^2}\right) \quad (2)$$

where $Q_{surf}$ is heat power of the plane heat source (17.3%) and R is the heat source radius. The radius of the heat source is calculated from the focal length of the focusing lens, which can be computed according to the relation found in [19]

$$R = \frac{2M_0^2\lambda F}{\pi D_0} \quad (3)$$

where $M_0^2$ is the value of beam quality (Nd:YAG laser with a wavelength (λ) of 1.060μm, beam quality is 1.04), F is the focal length of the focusing lens and $D_0$ is the minimum diameter of the laser beam (0.3mm). Assuming the simulation of keyhole is a cone, the Gaussian distribution of heat flux is written as [2]

$$Q(z) = \frac{2Q_{keyhole}}{\pi r_0^2 H} e^{1-\left(r/r_0\right)^2}\left(1-\frac{z}{H}\right) \quad (4)$$

where $Q_{keyhole}$ is the absorbed laser beam power (52%), $r_0$ is the initial radius (at the top of the keyhole - 0.3 mm), H is the sheet thickness, r is the current radius, i.e. the distance from the cone axis and z is the current depth. The total heat input to the model is computed from the summation of surface and volume heat source models.

*D. Discrete Model*

A numerical analysis of the transient temperature distribution during the laser welding process is performed using a finite element method. The model uses eight-node quadratic three dimensional solid elements. Since modeling of welding process involves temperatures above the boiling point of the material, the phase change is to be considered. This will be taken care by considering the enthalpy or latent heat of fusion of the material. The enthalpy E (heat energy per unit volume) is calculated from the equation proposed in [20]:

$$E = \int pCdT \quad (5)$$

The geometry and finite element mesh used in the models for simulating laser spot and seam welding to predict the temperature distribution and weld bead geometry are given in Fig. 8. Total number of nodes and elements are 49140 and 40000, respectively.

All the analyses are performed incorporating temperature dependent thermal properties of the base metal. The following assumptions are made in the formulation of the FE model:

1. The initial temperature of the workpiece is 30°C. Both the laser beam and mesh coordinates are fixed.
2. Thermal properties of the material like density, specific heat and conductivity are temperature-dependent.
3. The radiation and convection loads are taken into account by considering lumped heat transfer coefficient as proposed by [21].
4. The absorbed laser energy is considered as 69.3% of the beam power as proposed by [17].
5. The physical phenomena such as Maragoni effects, convective melt flow, buoyancy force and viscous force are neglected.

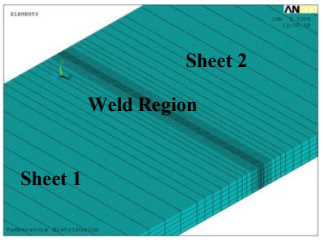


Fig. 8 Finite element mesh

*E. Butt Joint Simulation*

Laser butt welds are welds where two pieces of metal are joined at surfaces that are at 90° angles to the surface of at least one of the other pieces. The weld bead geometry describes how the metal pieces are fit together. In order to study the effect of the laser welding parameters on the weld bead geometry and the temperature field, a series of simulations over a range of welding conditions are performed.

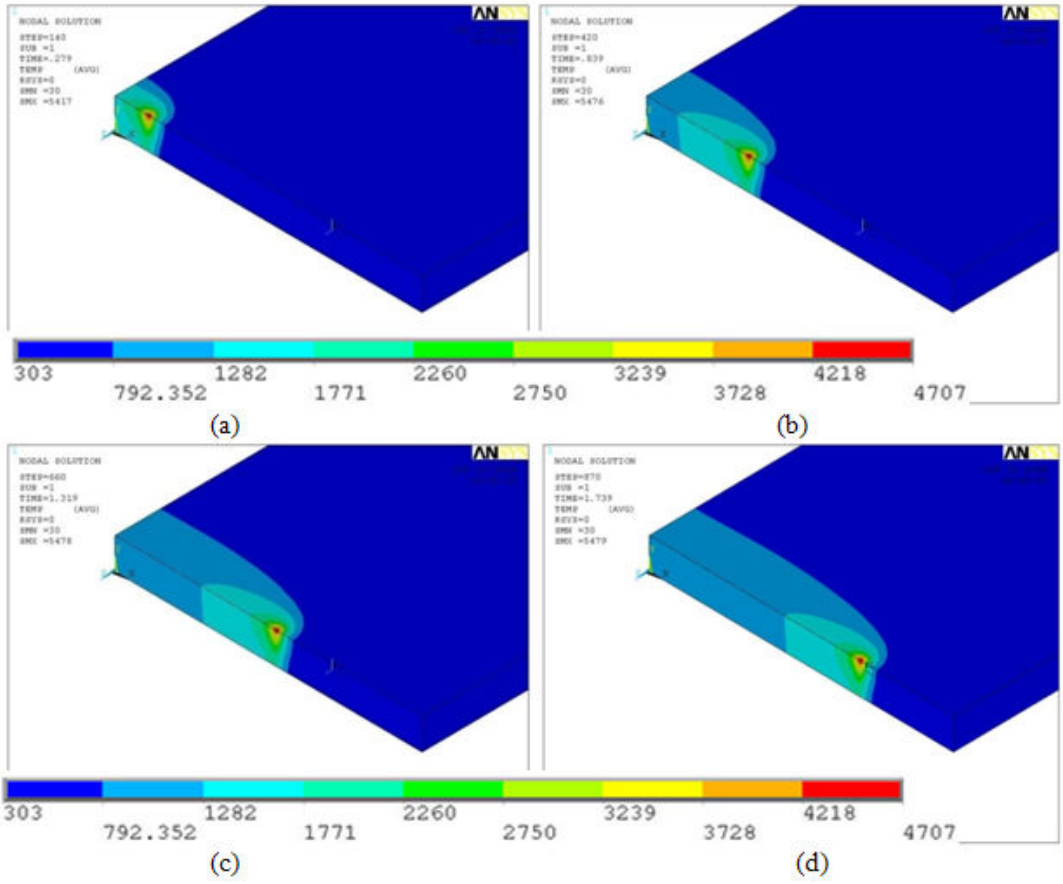


Fig. 9 Temperature distribution during welding process at four different times (a) 0.28 s, (b) 0.84 s, (c) 1.32 s and (d) 1.74 s

Fig. 9 shows the temperature distribution at four different times of the welding process for the 1800 W beam power, 800 mm/min welding speed and 85° beam incident angle. Fig. 10 shows temperature histories for selected nodes along the transverse plane to the weld direction. From this figure the severe temperature gradient during the heating analysis can be clearly noted. The figure clearly shows the presence of severe temperature gradient at the weld pool.

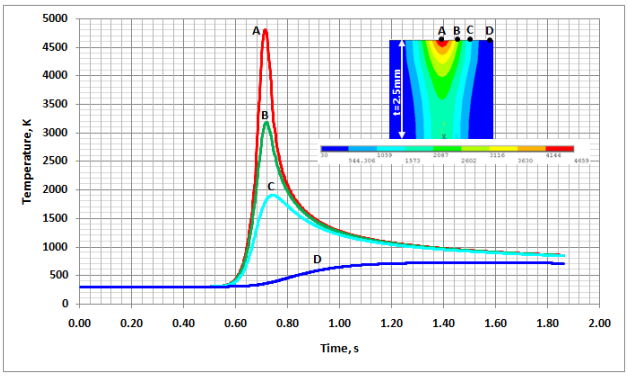


Fig. 10 Calculated temperatures for nodes A, B, C and D at various time steps

While the contour for the vaporization temperature (=2467°C) of the stainless steel defines the keyhole boundary, the region above the melting temperature (=1450°C) indicates the weld pool geometry (refer Fig. 11). Fig. 11 shows the temperature distribution around the keyhole on the top surface of the workpiece and along the cross section. It is observed that the weld pool is enlarged in the opposite direction of the welding speed.

This is due to the fact that there is a relative speed between the workpiece and the laser beam, the temperature gradient near the front wall of the keyhole is much greater than that near the rear wall of the keyhole. Hence, the part of the weld pool in front of the keyhole is very thin, while most part of the weld pool is located behind the keyhole. Moreover, the weld pool shape varies through the thickness due to the three dimensional character of the transient thermal field calculation.

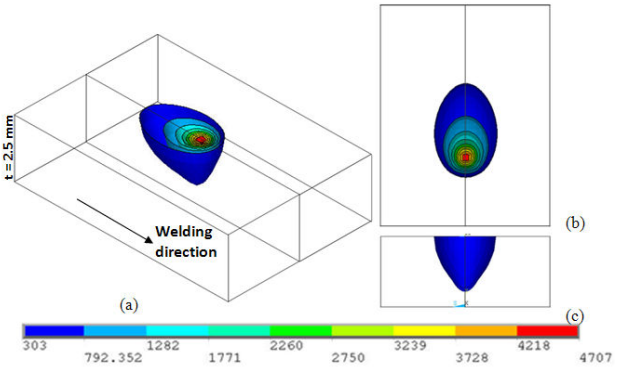


Fig. 11 Weld pool geometry (a) Weld pool isotherms, (b) Top view and (c) Weld cross section

Fig. 12 (a)-(f) show the effect of beam power on laser-weld bead geometry. It is noted that the dimensions of the bead have a significant change as the beam power is increased from 800 to 1,800 W for a constant welding speed of 800mm/min. In addition to that, an increase in beam power from 800 to 1,800 W shows a marked increase in penetration from approximately 0.86 (at 800 W) to 1.96mm (at 1,800 W).

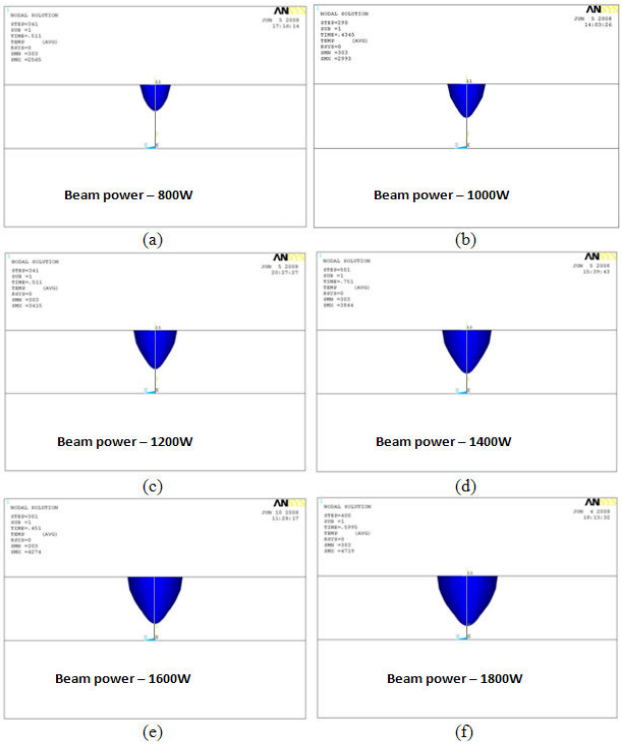


Fig. 12 (a)-(f) The effect of beam power on the bead geometry for the laser parameters: 800mm/min WS and 85° BA

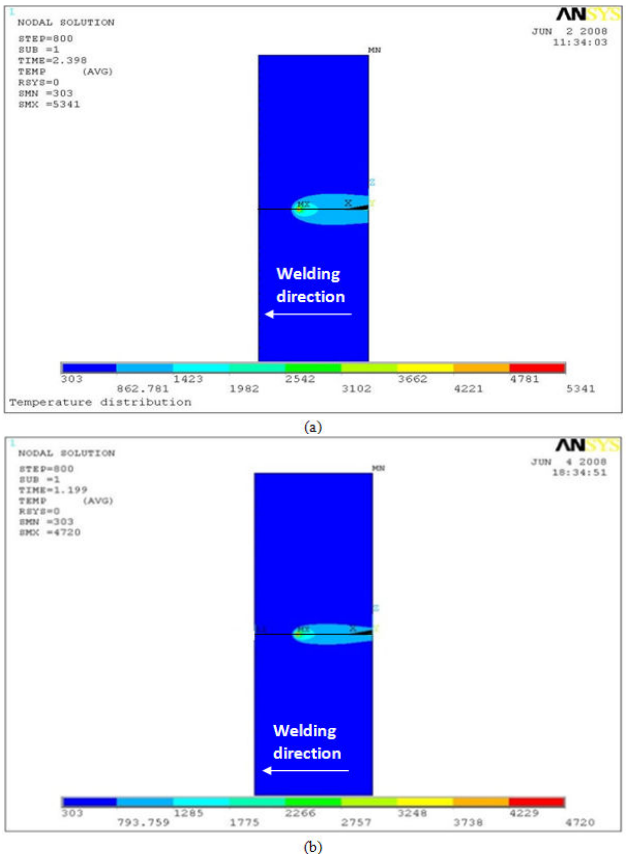

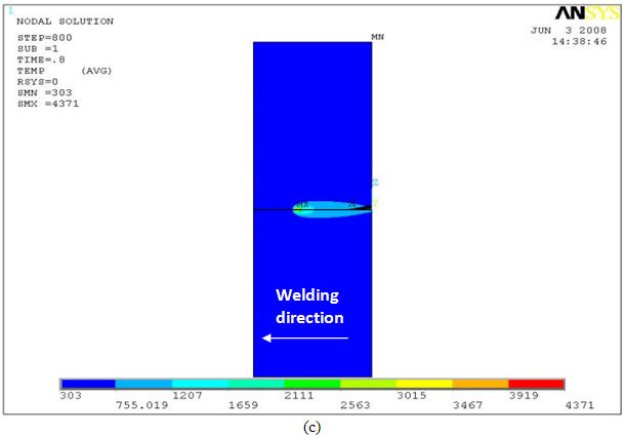


(c)

Fig. 13 Temperature profiles for three different welding speeds (a) 400mm/min, (b) 800mm/min and (c) 1200mm/min at 1800 W beam power and 85° beam incident angle – Load step no. 800

Similarly, there is also a slight increase in bead width from 0.9 (at 800 W) to 1.38mm (at 1,800 W). The possible reason may be that the power density distribution of the laser beam increases as the beam power increases, and it covers a wide area on the top surface of the sheet. Therefore, there is a slight increase in the bead width of the laser weld.

Fig. 13 shows the temperature distribution for three different welding speeds at load step no. 800. Results show that the temperature isotherms in front of the laser source are closer than those behind the source because of the convection effect of the welding speed movement. At very high welding speeds, the absorptivity of laser beam by the base metal is minimum (low interaction rate), which leads to low depth of penetration. Also there is some considerable reduction in bead width at high welding speed (1,200mm/min) compared to low welding speed (400mm/min) operated at constant beam power (1,800W) as shown in the Fig. 13.

Fig. 14 depicts the sizes of the molten pool as a function of welding speed at load step no. 800. Since the laser source moves, the molten pool shape is not circular as in the case of a stationary heat source. The elliptic nature of the pool shape is more prominent for the higher welding speed (1,400mm/min). As the reduction in the welding speed leads to increase in interaction time between the laser beam and base metal, which results in the increase of the peak temperature value (5,500K) and heat input along the thickness direction, causing a greater volume to be melted. As a result, the "heating tail" is longer and wider, leading to high depth of penetration. Under similar conditions, the increase of welding speed reduces both the peak temperature value (4,347K) and the heat conduction along the thickness direction, with a reduction of the molten pool volume [5]. This implies that a narrow fusion zone may be obtained as the welding speed increases.

The comparison of simulated molten zone form and dimension with those determined by metallurgical investigations are presented in Figs. 15 and 16. Fig. 15 depicts the complete penetration for the 2.5mm thick base metal obtained for a beam power of 1800 W at welding speed of 400 mm/min and bead incident angle of 85°.

Similar solidification profiles on the weldment top surface are noted comparing simulated temperature distribution near heat source and molten zone morphology (refer Fig. 16). There is a good correlation between the weld bead profile obtained by the finite element simulation and experiment result for the same welding parameters.

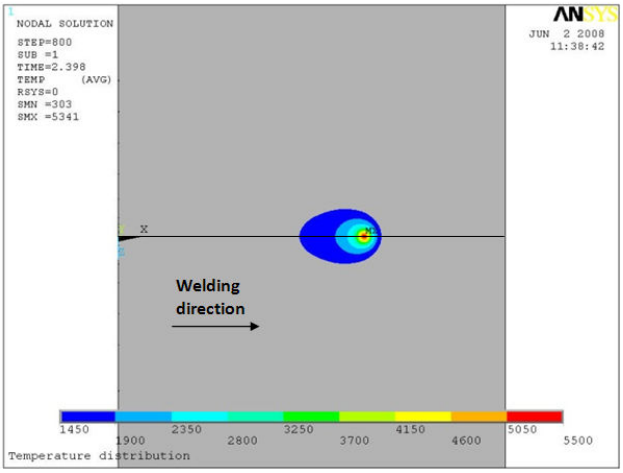


(a)

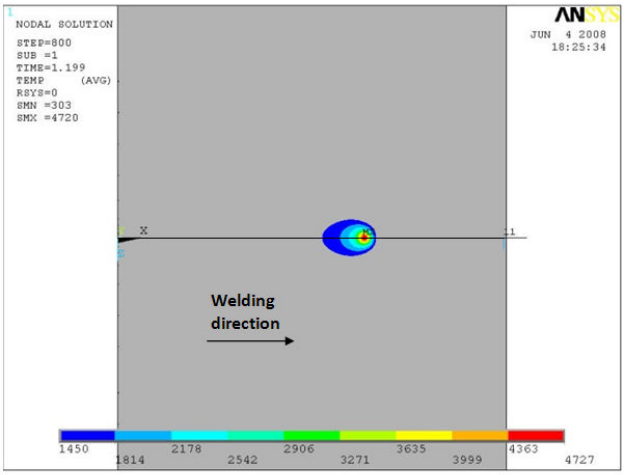


(b)

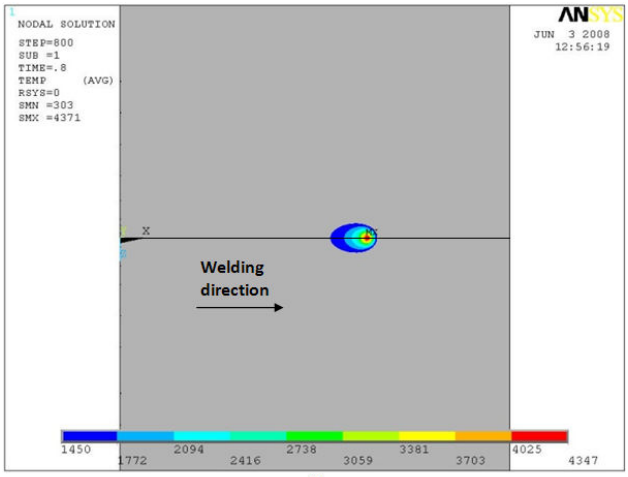


(c)

Fig. 14 Molten pool shapes for three different welding speeds (a) 400 mm/min, (b) 800mm/min and (c) 1200mm/min at 1800 W beam power and 85° beam incident angle – Load step no. 800

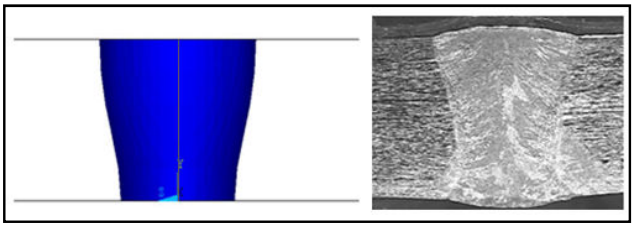

(a) (b)

Fig. 15 Weld bead profile from (a) FE simulation and (b) Experimental investigation

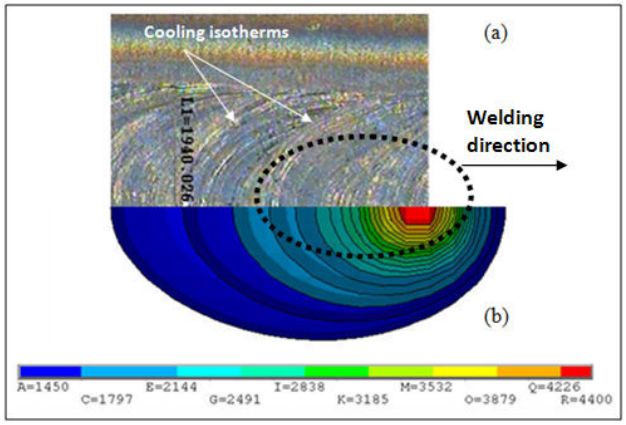


Fig. 16 Cooling isotherms from (a) FE simulation and (b) Experimental investigation

The weld bead shows the characteristic of laser welding with depth/width ratio close to 2. No welding cracks or porosity are found in the weld; this may be partly due to good crack resistance of the base metal and proper welding conditions being provided. The molten pool shapes obtained through simulation are similar to the experimentally measured bead shapes for all the combinations of laser parameters selected for the analysis and experimentation.

## IV. Conclusion

The present research article utilizes the finite element code ANSYS to investigate the temperature profiles and molten pool shape during the laser welding in butt-joint welds. The temperature dependent material properties for AISI304 stainless steel are taken into account in the calculation, which has a great influence in computing the temperature profiles. Based on the results of this investigation, the following conclusions are made:

- The distances between the center of the laser beam spot and the location where the peak temperature occurs increases slightly as the laser power is increased, but decrease with increase of the welding speed. For all the welding conditions, the temperature peaks are at the "heel" of the center of the laser source.
- The elliptic nature of the molten pool shape is more prominent in the case of higher welding speed (1400mm/min). The increase of welding speed reduces the peak temperature value and the heat conduction along thickness direction, with a reduction of the molten pool volume.
- A series of experiments have been conducted to validate the finite element simulation results, the quality of laser welds is good, since no phenomena such as warpage, porosity, etc. are present
- The computed temperature profiles and molten pool shapes are observed to be in correlation with the experimental measurements.

## Acknowledgment

The authors thank Head and Management of Welding Research Institute (WRI), Bharat Heavy Electricals Limited, Tiruchirappalli, India for extending the lab facilities to carry out this research work and allowing to present the results in this paper. Authors thank NITT for providing computation facilities (ANSYS).

## References

[1] J.F. Ready and D.F. Farson, "*LIA Handbook of Laser Materials Processing*", 1st ed., Magnolia Publishing, Laser Institute of America, 2001.
[2] S.A. Tsirkas, P. Papanikos and Th. Kermanidis, "Numerical simulation of the laser welding process in butt-joint specimens", *Journal of Materials Processing Technology,* 134, pp 59-69, 2003.
[3] D. Rosenthal, "The Theory of Moving Source of Heat and it's Application to Metal Treatment", *Trans. ASME,* 68, pp. 849–866, 1946.
[4] D.T.S. Hook and A.E.F. Gick, "Penetration welding with lasers", *Welding Research Supplement*, pp. 492s-498s, 1973
[5] M. Lax, "Temperature rise induced by a laser beam", *Journal of Applied Physics*, 48, pp. 3919-3924, 1977.
[6] J. Dowden, M. Davis and P. Kapadia, "Some aspects of the fluid dynamics of laser welding", *Journal of Fluid Mechanics*, 126, pp. 123-146, 1983.
[7] R. Brockmann, K. Dickmann, P. Geshev and K. J. Matthes, "Calculation of temperature field in a thin moving sheet heated with laser beam", *International Journal of Heat and Mass Transfer*, 46, pp. 717-723, 2003.

[8] A. Mahrle and J. Schmidt, "The influence of fluid flow phenomena on the laser welding process", *International Journal of Heat and Fluid Flow*, 23, 288-297, 2002.
[9] A.P. Mackwood and R.C. Crafer, "Thermal modelling of laser welding and related processes: literature review", *Optics & Laser Technology*, 37(2), pp. 99–115, 2005
[10] K.Y. Benyounis, A.G. Olabi and M.S.J. Hashmi, "Effect of laser welding parameters on the heat input and weld-bead profile", *Journal of Materials Processing Technology*, 164–165, pp. 978–985, 2005.
[11] H. GuoMing, Z. Jian and L. JianQang, "Dynamic simulation of the temperature field of stainless steel laser welding", *Materials & Design*, 28(1), pp. 240-245, 2007.
[12] D. Radaj, "*Heat Effects of Welding, Temperature Field, Residual Stress, Distortion*", Springer-Verlag, Berlin, Heidelberg, New York, London, Paris, Tokyo, 1992.
[13] Z. Ji and S. Wu, "FEM Simulation of the temperature field during the laser forming of sheet metal", *Journal of Materials Processing Technology*, 74(1-3), pp. 89-95, 1998.
[14] J. Sabbaghzadeh, M. Azizi and M.J. Torkamany, "Numerical and experimental investigation of seam welding with a pulsed laser", *Journal of Optics & Laser Technology,* 40, pp. 289-296, 2008.
[15] W.S. Chang and S.J. Na, "Prediction of laser spot weld shape by numerical analysis and neural network", *Metallurgical and Material Transactions B,* 32B, pp 723-731, August 2001.
[16] C.S. Wu, H.G. Wang and Y.M. Zhang, "A New Heat Source Model for Keyhole Plasma Arc Welding in FEM Analysis of the Temperature Profile", *Welding Journal*, 85(12), pp. 284s-291s, 2006.
[17] J. Xie and A. Kar, "Laser Welding of Thin Sheet Steel with Surface Oxidation", *Welding Research Supplement,* 78, pp. 343s – 348s, 1999.
[18] C. Carmignani, R. Mares and G. Toselli, "Transient finite element analysis of deep penetration laser welding process in a singlepass butt-welded thick steel plate", *Journal of Computational Methods in Applied Mechanics and Engineering,* 179, pp. 197-124, 1999.
[19] W.R. Harp, A.G. Paleocrassas and J.F. Tu, "A Practical method for determining the beam profile near the focal spot", *International Journal of Advanced Manufacturing Technology*, 37(11-12), pp. 1113-1119. 2007.
[20] ANSYS® Release 9.0 Documentation *Chapter 3.9 Phase Change* (data accessed on 29.01.2009)
[21] M.R. Frewin and D.A. Scott, "Finite Element Model of Pulsed Laser Welding", *Welding Research Supplement*, 78, 15s-22s, 1999.

**Nallathambi Siva Shanmugam** was born in Tiruchirappalli, INDIA on 16 November 1980. He received his Bachelor degree in Mechanical Engineering from Bharathidasan University, INDIA in 2002. He was awarded Master degree in CAD/CAM from Anna University, INDIA in 2004. He received his Doctoral degree in Finite Element Simulation pertaining to Laser Beam Welding process from National Institute of Technology (NIT) Tiruchirappalli, INDIA in 2012. His field of interest includes Finite Element Simulation on Laser Beam Welding, Friction Stir Welding, TIG welding and Bio-Mechanical Engineering.

**Gengusamy Buvanashekaran** received his integrated M.S. (Engg.) in Welding Technology from Slovak Technical University (SVST), BRATISLAVA in 1981 with honours. In 1995 he obtained his Ph.D on Submerged Arc Welding fluxes from Bharathidasan University, INDIA. Presently, he is working as an Additional General Manager at Welding Research Institute (WRI), BHEL, INDIA. His research interest encircles - the area of High Energy Beam processes like LASER and ELECTRON BEAM.

**Krishnasamy Sankaranarayanasamy** is Professor of Mechanical Engineering at National Institute of Technology Tiruchirappalli, INDIA received his B.E (Hons) in 1981 from PSG College of Technology, INDIA. He received his M.Tech in 1983 and Ph.D in 1989 from Indian Institute of Technology Madras, INDIA. His area of research mainly focuses on Laser Materials Processing, Industrial safety and Optimization in Design.